The Iranian Journal of Mechanical Engineering Transactions of ISME
Journal homepage: https://jmee.isme.ir
Vol. 24, No. 1, 2023, pp. 85-98

Research Paper

DOI: https://doi.org/10.30506/jmee.2023.562384.1299
DOR: https://dorl.net/dor/20.1001.1.16059727.2023.24.1.6.0

Experimental Study of Parameters Affecting Friction Reduction in Solid-Liquid Interfaces using Ultrasonic Vibrations

Ali Fattahi Avati*
M.Sc.

Mohammad Reza Karafi †
Assistant Professor

The utilization of ultrasonic waves is a method to reduce frictional drag. Available hypotheses state that ultrasonic vibrations reduce frictional drag by creating cavitation, forming a fluid vapor layer surrounding the surface, and reducing its contact surface. This paper examines the hypothesis by performing experimental tests to eliminate the cavitation effect via increasing the pressure and investigates other factors affecting the frictional drag reduction. Experimental tests showed that by applying ultrasonic vibrations, frictional drag is reduced by an average of about 9%. Besides, by eliminating the cavitation effect, the frictional drag reduction is nearly 6%. It reveals that about 3% of frictional drag reduction was related to cavitation. The shear stress relation shows that the effect of variation of shear surface and distance in the presence of ultrasonic vibrations are negligible, and therefore the only factor that affects the drag force reduction is viscosity. It can be hypothesized that ultrasonic vibrations reduce viscosity by mechanisms such as increasing both local temperature and the distance between molecules. The tests showed that the viscosity was reduced by 6% by using ultrasonic waves.

Keywords: Ultrasonic, Frictional Drag, Cavitation, Viscosity

1 Introduction

Today, the use of ultrasonic waves in different industries has been extensively progressed. The applications of the ultrasonic waves include medicine, cleaning, welding of metals and plastics, water purification, ultrasonic sewing, stress-relief of industrial components, forming processes, fluids spray in semi-conductors' production, homogenizing nano-powder, and food industries

* M.Sc., Faculty of Mechanical Engineering, Tarbiat Modares University, Tehran, Iran, ali.fattahi@modares.ac.ir
† Corresponding Author, Assistant Professor, Faculty of Mechanical Engineering, Tarbiat Modares University, Tehran, Iran, karafi@modares.ac.ir

Received: 2022/10/30, Revised: 2023/04/04, Accepted: 2023/09/25

[1-8]. An important application of ultrasonic vibrations is friction reduction. Shahgholian et al. [9] performed an experimental study to investigate the effect of ultrasonic vibrations on the friction force. Their results show that the reduction of friction force due to ultrasonic vibrations in different conditions is in the range of 40-100%. In addition, a severe reduction in friction force was observed as the velocity of vibrations is increased. Ultrasonic vibrations are used in Enhancement Oil Recovery (EOR) processes. Applying the ultrasonic waves results in a friction reduction between oil and stones' cavities of well. As a result, the oil flows toward the perforation zone of a well [10]. The effect of ultrasonic waves to improve rheological and qualitative indexes of heavy gasoline flow was studied by Gopinath et al. [11]. They used waves at the atmosphere pressure without adding any solvent. In addition, they used an ultrasonic transducer with a frequency 20 kHz and the maximum power of 1500W. The samples were tested at vibration amplitudes of 30, 40, 50, 60, and 70 microns and 5-20 minutes of radiation time. The lighter gaseous hydrocarbons such as methane, ethane, ethylene, and propylene were extracted during the radiation of waves. The nitrogen components were easily decomposed using the cavitation energy. Ruirun et al. [12] investigated the effect of ultrasonic vibrations on the microstructure and mechanical properties of Al-Ti alloy in the casting process. The results revealed that the coarse-grained microstructure is converted to a fine-grained spherical structure with a homogeneous distribution of components and small sedimentary particles. The ultrasonic waves are used to create cavitation layers on floating boundaries in fluids in order to reduce the drag force [13]. The forces acted on a floating body in a fluid are divided into two categories. The first force, called pressure drag, is due to the fluid mass. This force depends on the fluid type and density and cannot be reduced for a flowing fluid. The second force is a frictional drag. By applying ultrasonic vibrations, a thin layer of fluid vapor is formed. It is evident that the wider vapor film formed on a fluid-solid interface, the lower the frictional drag; the reason for this is related to lower shear stress tolerated by the vapor.
In the present study, a laboratory setup has been designed and built to investigate the effect of ultrasonic vibrations on lowering the frictional drag in the absence of cavitation. In this research, the cavitation has been removed by increasing a tank pressure, and the other factors affecting the drag reduction are investigated.

2 Principle

The frictional drag is a part of the drag force related to the fluid's shear stress applied to the body surface [14]. Fig. (1) shows the deformation of fluid under the shear stress.
Shear stress is expressed as follows:

$$\tau = \mu \frac{du}{dy} \tag{1}$$

where, μ is the viscosity of the fluid, and u is velocity.

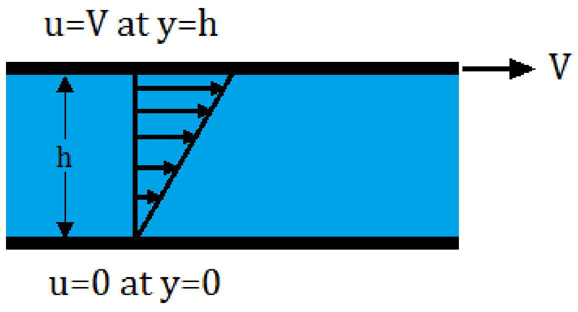

Figure 1 Fluid shear stress between two planes

2.1 Cavitation

Cavitation is a phenomenon in which the vapor bubbles are formed in low-pressure regions of the fluid, and are collapsed in high-pressure regions. The cavitation phenomenon is the same as the liquid boiling, but the difference is that boiling occurs due to the temperature rise while the cavitation occurs due to the pressure drop. The water vapor is formed when the pressure is reached 2.33×10^{-2} bar at a temperature of 20 ℃.

2.2. Elimination of cavitation

Fig. (2) represents a flat surface of an acoustic radiator with a radius of a, which oscillates with the velocity of $v_0\exp(j\omega t)$.
The product of the acoustic impedance times the velocity can be used to calculate the pressure in every point of the space [15]:

$$P(r,\theta,t) = j\rho c\frac{v_0}{\lambda}\int_S \frac{1}{r'}e^{j(\omega t-kr')}dS \tag{2}$$

where, ρ and c are the fluid density and sound speed in fluid, respectively. The integral is applied for $\sigma \le a$. Solving this integral for an arbitrary point is very difficult. However, the integral can be solved in a closed form for two cases: (a) along a line perpendicular to the surface passing its center; (b) far from the surface.
The calculation of field along the z-direction is in the following form:

$$P(r,0,t) = j\rho c\frac{v_0}{\lambda}e^{j\omega t}\int_0^a \frac{exp\left(-jk\sqrt{r^2+\sigma^2}\right)}{\sqrt{r^2+\sigma^2}}2\pi\sigma d\sigma \tag{3}$$

By solving the integral, the pressure is calculated as follows:

$$P(r,0,t) = \rho c v_0\left\{1-exp\left[-jk\left(\sqrt{r^2+a^2}-r\right)\right]\right\}e^{j(\omega t-kr)} \tag{4}$$

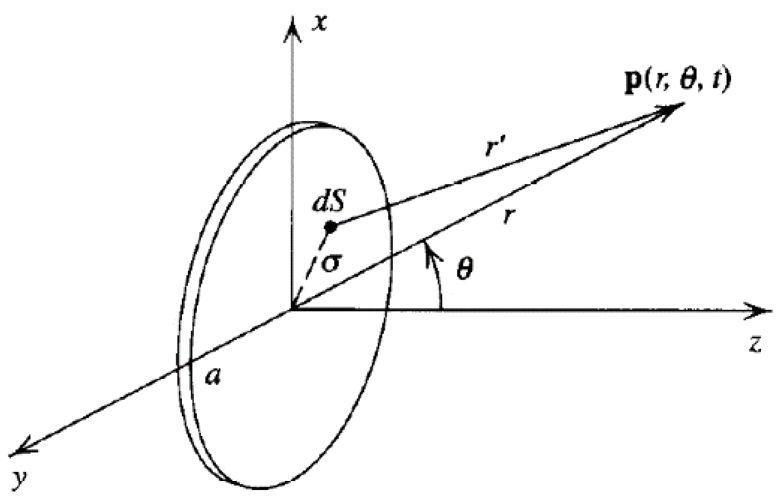

Figure 2 The surface of an acoustic radiator

The pressure amplitude on the surface axis is calculated as:

$$P(r,0) = \rho c v_0 \left| 2sin\left\{\frac{1}{2}kr\left[\sqrt{1+({}^{a}/_{r})^2}-1\right]\right\}\right| \tag{5}$$

where $k = \frac{2\pi}{\lambda}$ is the wave number. By substituting the wave number in Eq. (5), the following equation is obtained for the pressure amplitude distribution.

$$P_A(r) = \rho c v_0 \left| 2sin\left(\frac{\pi}{\lambda}(\sqrt{r^2+a^2}-r)\right)\right| \tag{6}$$

where $P_A(r)$ is the pressure amplitude at the distance r from the booster's tip. Besides, v_0, λ and a are velocity amplitude of the booster's tip, sound's wavelength in the fluid, and booster's tip radius. Water, with a density of 1000 kg/m^3, was used as the working fluid in this research. The wavelength is calculated by Eq. (7).

$$\lambda = \frac{c}{f} \tag{7}$$

where $f = 20\ kHz$ is the frequency, and $c = 1418\ m/s$ is the sound speed in the water. Thus, the wavelength in water is equal to 0.071 m.
In this test, $a = 9mm$ and based on the 5-micron oscillations, $v_0 = 0.314 m/s$. The pressure amplitude on the booster's head (r=0) is equal to 3.45 bar using Equation (6). Also, the pressure amplitude at the maximum distance between the moving object and booster's head ($r = 1\ mm$) is 3.1 bar.
According to Fig. (3), pressure oscillations are created in the fluid due to vibrations, and since the water vapor pressure at a temperature of 20℃, is 0.02 bar, cavitation is created at negative pressure zones. Thus, by applying a pressure higher than 3.47 bar, the minimum pressure will be higher than the water vapor pressure; as a result, the cavitation is not formed.
In this research, constant pressure has been created inside a chamber using a 16 bar manual water pump. The manual water pump has two one-way valves that keep the pressure inside the chamber constant at desired values.
In the following, the effect of ultrasonic vibrations on different parameters of the shear stress is investigated theoretically. Firstly, the effect of vibrations on the parameters of the shear stress has been studied by assuming a constant viscosity. The shear force can be calculated using Eq. (8):

$$F = \tau A \tag{8}$$

The shear-affected area of a booster shown in Fig. (4) is calculated by Eq. (9).

$$A = A_1 + A_2 \tag{9}$$

where the vertical area of the booster can be calculated by Eq. (10).

$$A_1 = 2\pi(r_0 + r\,sin(\omega t))(l_0 + l\,sin(\omega t)) \tag{10}$$

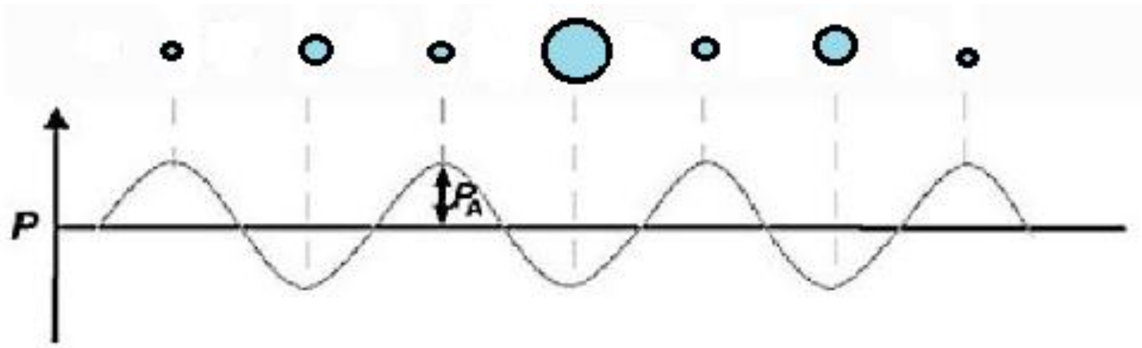

Figure 3 Formation of cavitation by pressure oscillations

and, the horizontal area of the booster is calculated by Eq. (11).

$$A_2 = \pi d_0^2/4 \tag{11}$$

Shear stress in the presence of vibrations in the area A_1 is obtained as:

$$\tau_1 = \mu \frac{\Delta V}{\Delta h} = \mu \frac{V}{h_0 + r\sin(\omega t)} \tag{12}$$

The following equation is used to calculate the average shear force under ultrasonic vibrations.

$$\overline{F_1} = \frac{1}{T}\int_0^T \tau_1 A_1 \, dt \tag{13}$$

Where T is the period of vibrations. To calculate the average resistive torque of the shaft from the area of A_1, Eq. (14) is used.

$$\overline{M_1} = \overline{F_1} r_0 \tag{14}$$

Shear stress in the presence of vibrations in the area A_2 is obtained as:

$$\tau_2 = \mu \frac{\Delta V}{\Delta h} = \mu \frac{r\tilde{\omega}}{h_1 + l\sin(\omega t)} \tag{15}$$

Where $\tilde{\omega}$ and ω are the angular velocity of the rotating shaft and the frequency of vibrations respectively. To calculate the resistive torque of the shaft from the area of A_2, Equation (16) is used.

$$M_2(t) = \int_0^{d_0/2} \mu \frac{\tilde{\omega}}{h_1 + l\sin(\omega t)} 2\pi r^3 \, dr \tag{16}$$

The following equation is used to calculate the average resistive torque of the area A_2.

$$\overline{M_2} = \frac{1}{T}\int_0^T M_2(t)\,dt \tag{17}$$

Fig. (4) represents parameters and surfaces used in the equations.
The values listed in Table (1) have been used to calculate the average resistive torque in the presence of ultrasonic vibrations. The Reynolds number in the test is calculated as 180. The value of the torque before applying vibrations was 2.48 μNm.

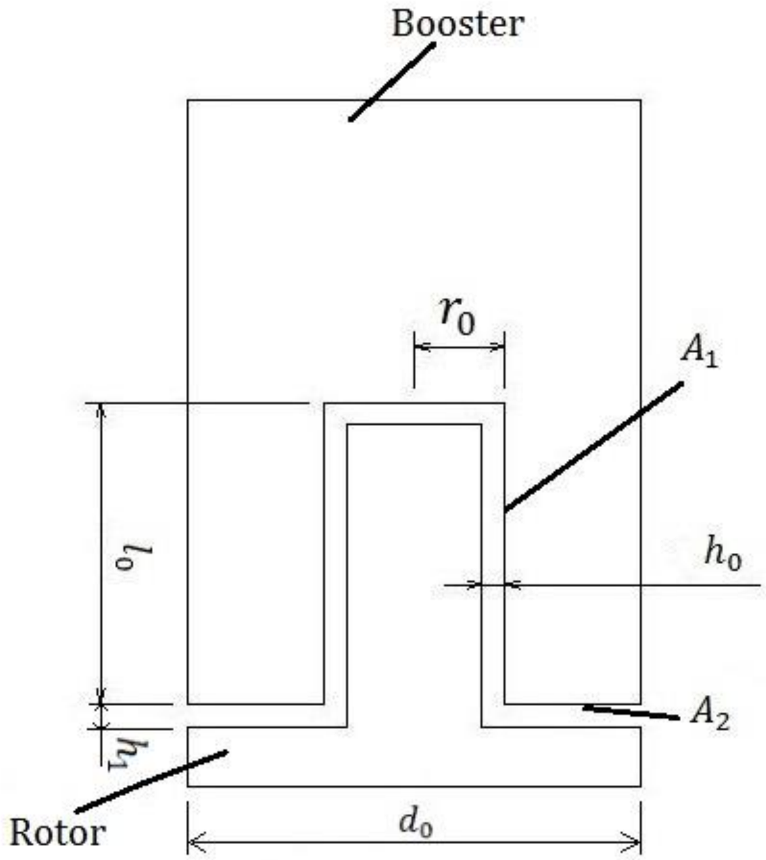

Figure 4 Rotor-booster contact surfaces

Table 1 Values used for calculating resistive torque

parameter	description	value	unit
h_0	Distance between two planes	1.5	mm
h_1	Distance between two planes	1	mm
r	Radial vibration amplitude	1	μm
r_0	Booster's hole radius	6	mm
l_0	Booster's hole length	20	mm
l	Longitudinal vibration amplitude	5	μm
d_0	Booster's forehead diameter	30	mm
μ	viscosity	$1.003*10^{-3}$	$N.s/m^2$
$\widetilde{\omega}$	Angular velocity of the rotating shaft	1600	rpm
ω	Frequency of vibrations	125663.7	Rad/s

With the use of values of Table (1), the average of the resistive torque in the presence of oscillation terms is near zero. The obtained reduction was very lower than the drag force reduction measured in the experimental test. So, the reduction of viscosity might be the main factor causing the drag force reduction.

3 Experimental setup

Drag force is created when a rigid body moves inside a fluid. The present research aims to study the effect of parameters other than the cavitation on the reduction of the drag force. To this end, the fluid pressure should be kept at the level to prevent cavitation. For measuring the frictional drag applied to a body, the torque applied to a rotating shaft can be used. The consumed current of the motor has been used to estimate the drag force. With increasing the torque applied to the shaft, the motor current is increased. The consumed current has been accurately measured using a KYORITSU KEW1008 multimeter manufactured in Japan. The accuracy of the ampere meter is 1 mA. The experimental setup is shown in Fig. (5). The pressure tank in the experimental setup is shown in Fig. (6). A cross section view of the test chamber is shown in Fig. (7).

3.1 Rotating body

The rotating body should be positioned such that the ratio of frictional drag to pressure drag becomes maximum. Figs. (6) and (7) show the rotating body and its position near the booster, respectively. The booster is fasten on the top of the tank with an O-ring. The rotor is connect to the tank using two ball bearings and a seal. The electromotor is fixed and its rotor rotates inside the tank. Angular velocity of the motor is measured with a cyber tech digital photo laser tachometer. The pressure of the test chamber is measure by a 10 bar Niigata Seiki pressure gage, Japan. The accuracy of the pressure gauge is 2% FS.

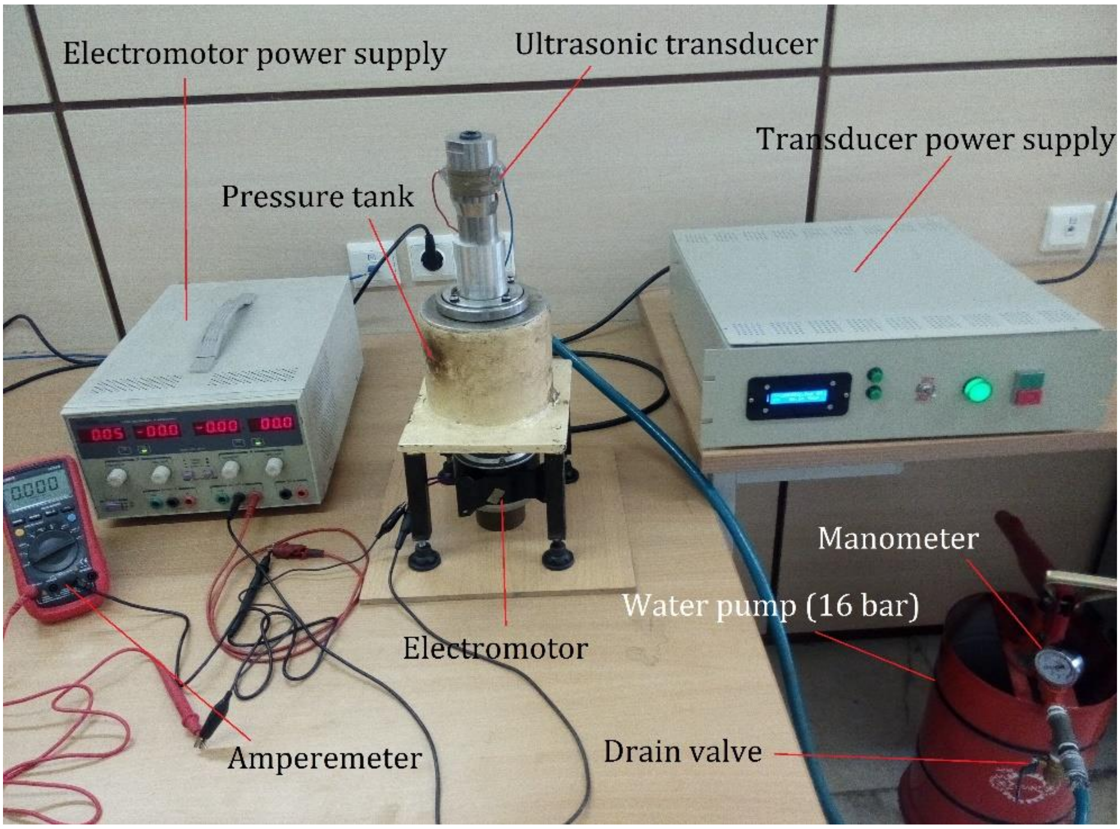

Figure 5 Experimental setup to measure frictional drag

(a)

(b)

Figure 6 (a) rotor, (b) rotor's position in the tank

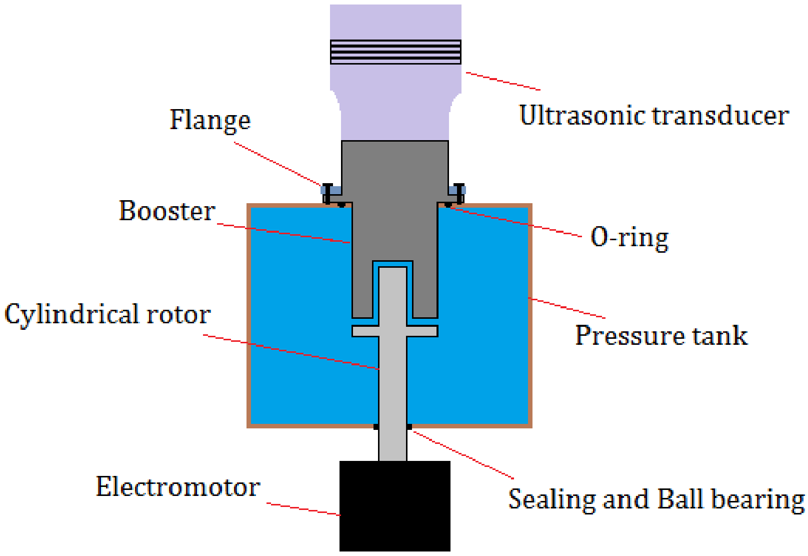

(a)

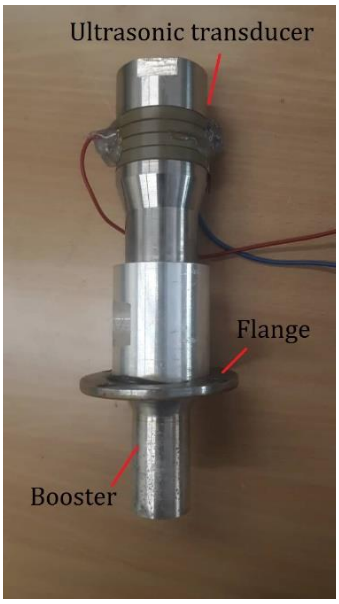

(b)

Figure 7 (a) cross section view of the test chamber (b) ultrasonic transducer and booster

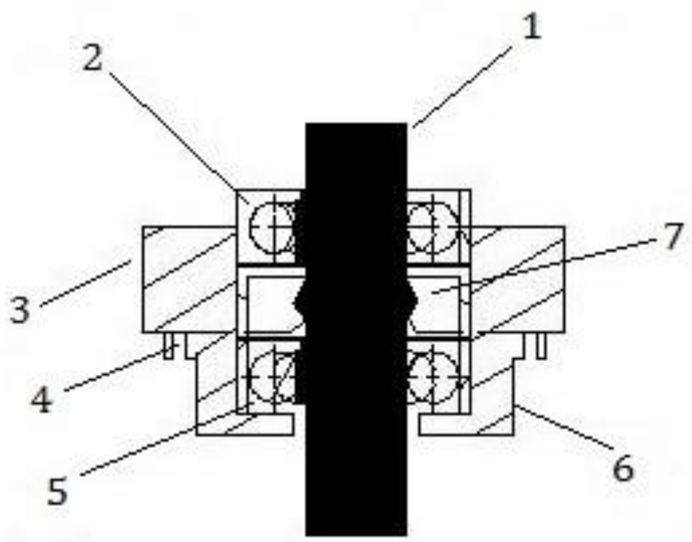

Figure 8 The sealing mechanism used in the test

(1) Rotating shaft; (2) upper ball bearing; (3) tank wall; (4) screw hole connecting ball bearing seat to the tank; (5) lower ball bearing; (6) ball bearing seat; (7) seal

A piezoelectric Langevin ultrasonic transducer with the resonant frequency of 20.05 kHz, bandwidth of 200 Hz, and maximum power of 2 kW is used. The transducer is excited by the ultrasonic power supply of ULPS2000 manufactured in IRAN, Alfa Co. with the maximum power of 2kW, and frequency range of 17 through 27 kHz. Amplitude of the tip of the booster is 5 microns. The lateral vibration amplitude is 1 micron. The amplitudes are measured by an eddy current gap sensor of AEC 5509, applied electronics Japan, with a precision of 0.2 micrometers and a bandwidth of 30 kHz. Power consumption duration the tests is 600W. This power is kept constant via the power supply. The power measure by the power supply with the accuracy of 1W.

3.2 Sealing system

A high pressure seal is used to prevent the leakage of fluid and prevents the penetration of particles into the enclosure. Teflon is used in this type of seal to prevent wear. These seal are of double-edged types and have high resistance against tearing, wear, and sudden impacts.
Two ball bearings have been used upper and lower of the seal to prevent vibrations of the motor shaft during the rotation as well as to prevent damaging of the sealing system. Fig. (8) show the sealing mechanism used in the test.

4 Results and discussions

The motor current in the absence of fluid and the speed of 1600 rpm is 0.88A. The relation between current and torque of a DC motor is as follow:

$$T_m = \frac{60KI\varphi}{2\pi} \tag{18}$$

Where T_m, K, I, φ are torque, motor constant, armature current and flux generated by permanent magnets, respectively. Also the torque of the motor is proportional to the consumed current.

As can be seen from Fig. (9), with increasing the speed, the drag force is increased, while by applying ultrasonic vibrations, the drag force decreases. At a constant speed and pressure, the consuming current of the motor under the exposure of ultrasonic waves is smaller than the condition without ultrasonic waves.
According to theoretical calculations, at pressure higher than 3.5 bar, the cavitation has been totally vanished. Fig. (9) reveals that utilization of ultrasonic vibrations led to a reduction in the frictional drag even without cavitations. To study the effect higher pressure, Fig. (10) shows the variation of the motor current versus the pressure at the speed of 1600 rpm.

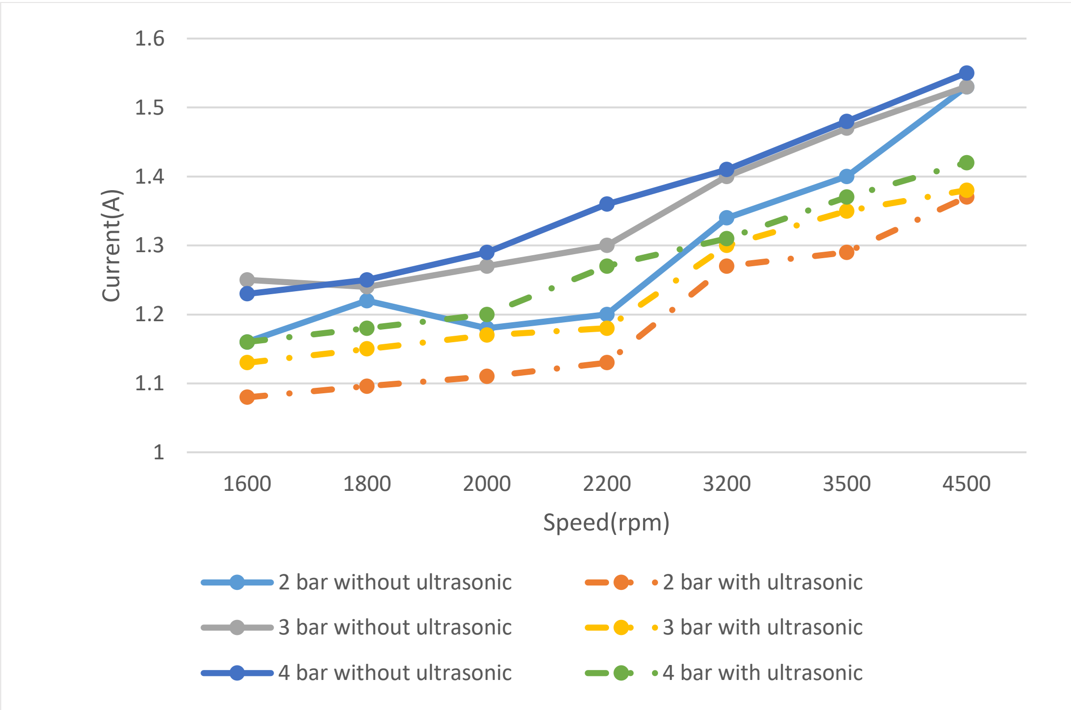

Figure 9 Variation of motor current versus speed with/without ultrasonic vibrations

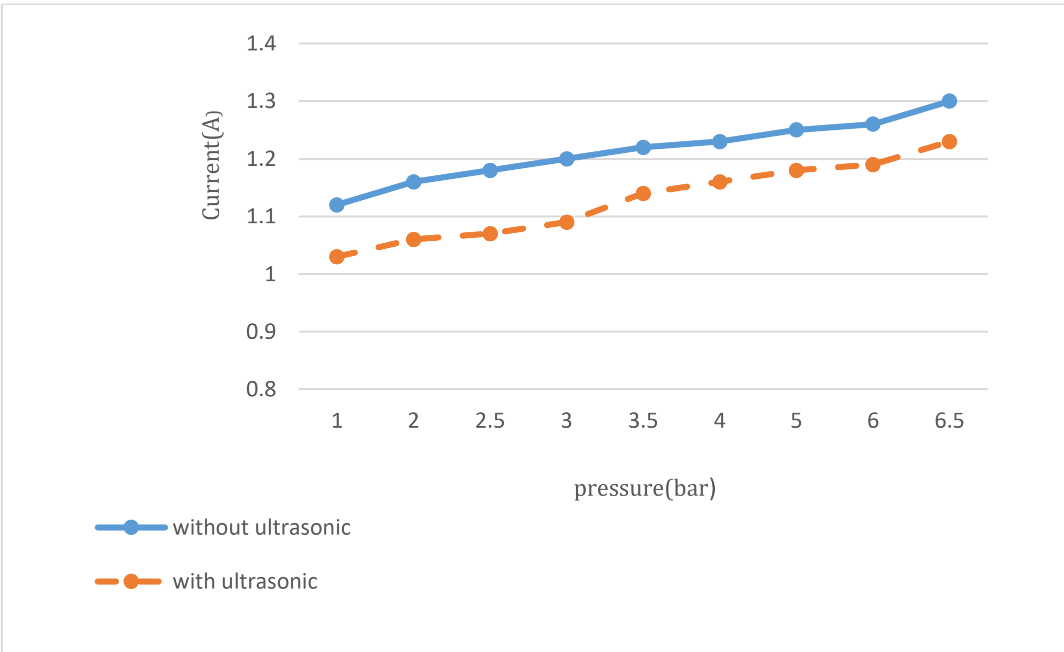

Figure 10 Variation of the motor current versus the pressure at the speed of 1600 rpm

For pressure higher than 3.5 bar, the reduction is reduced which may be due to the lack of cavitation. At pressures higher than 3.5 bar, the cavitation does not exist; however, a reduction in frictional drag is observed. For example, at the speed of 1600 rpm, the average reduction is 9% from zero to 3 bar. But the average reduction is 6% from 3.5 through 6.5 bar. It means that about 3% of the reduction is related to the cavitation. The drag force reduction versus the fluid pressure is shown in Fig. (11).
The temperature increase is one of the most important factors in the viscosity reduction. The utilization of ultrasonic vibrations can increase the local temperature of the fluid. Another significant reason why ultrasonic vibrations affect viscosity is their effect on the molecular structure of the material. The molecules in materials are bonded by the Van der Waals force. This force varies in terms of intermolecular distance. Fig. (12) is depicted to show the Van der Waals force in terms of intermolecular force.

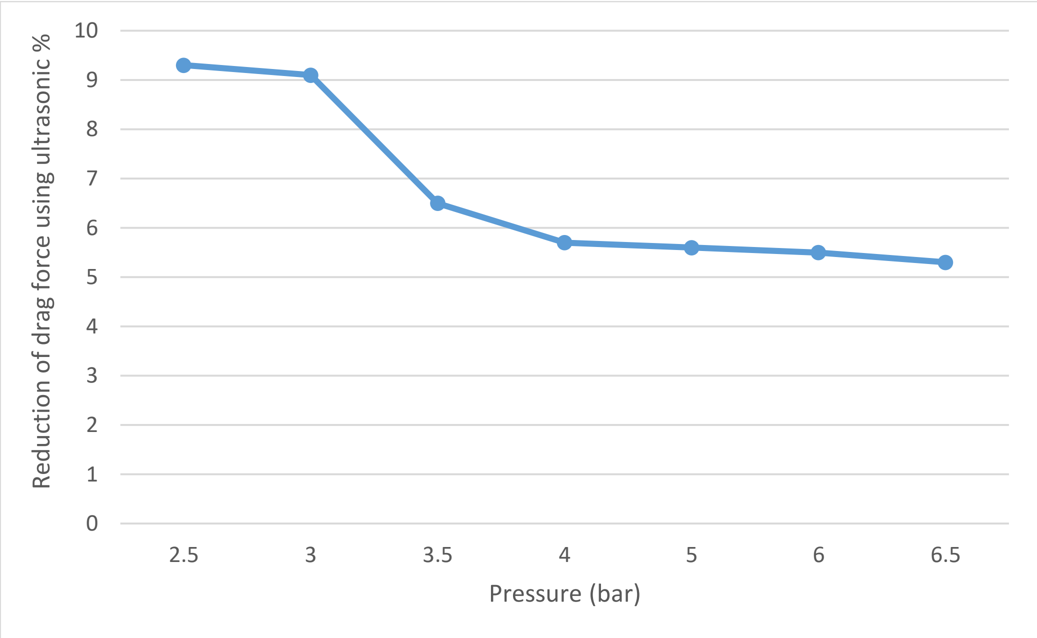

Figure 11 The drag force reduction versus the fluid pressure at the speed of 1600 rpm

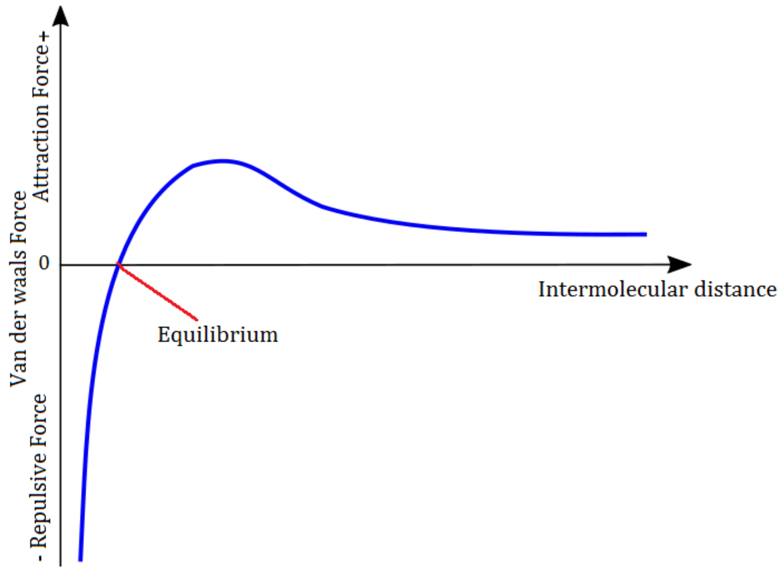

Figure 12 Van der Waals force in terms of intermolecular distance

According to Fig. (12), if the molecules' distance from the equilibrium point is increased, the attraction force is created, and molecules are attracted. On the other hand, if the molecules get closer to each other, the repulsive force is increased. Naturally, the molecules oscillate around their equilibrium point, and this oscillation generally occurs at high frequencies (up to the frequency of infrared waves). When ultrasonic vibrations are applied to a media, the oscillations of molecules are increased. These oscillations are not symmetric because the attraction force is lower than the repulsive ones, so the molecules tend to get away due to these vibrations. As a result, the average equilibrium distance is increased. This increased distance results in lowering intermolecular adhesion, as well as viscosity. Increasing the temperature will increase molecules' vibrations and their intermolecular distance; this will result in less intermolecular adhesion or reduced viscosity. Therefore, it can be concluded that the viscosity reduction is a possible reason for the frictional drag reduction in the absence of the cavitation. Both ultrasonic waves and temperature can create movements of molecules and therefore increase the distance between them. However, the temperature rise due to viscoelastic losses of the fluid is occurred slowly than the effect of ultrasonic waves. Hence the first reason to increase the molecular distance is mechanical vibrations, and after that passing wave may loss energy and increase the temperature.

5 Conclusion

In fluid-solid surface, different parameters affect the frictional drag, including viscosity, speed, shear planes' distance, and shear area. Applying oscillation terms reveals that the existence of vibrations in the shear surface and the shear planes' distance has no significant effect on the shear stress. It was observed that viscosity is the only factor that causes a reduction in shear stress. By removing the cavitation, utilization of ultrasonic waves has led to a viscosity reduction, resulting in the frictional drag reduction. According to the tests performed in the present research, the effects of viscosity and cavitation on the frictional drag reduction are 6%, and 3%, respectively for the experimental conditions of this research.

6 Declarations

6.1 Competing Interests

We declare that we have no significant competing financial, professional, or personal interests that might have influenced the performance or presentation of the work described in this manuscript.

6.2 Availability of data and materials

Raw data were generated at Metrology and Advanced Mechatronics Laboratory, faculty of mechanical engineering, Tarbiat Modares University, Tehran, IRAN. Derived data supporting the findings of this study are available from the corresponding author on request.

6.3 Authors contributions

Ali Fattahi performed experiments, collected data, wrote a draft of the paper. Mohammad Reza Karafi analyzed the data, organized and revised the paper.

6.4 Ethical Approval

This declaration is "not applicable".

6.5 Funding

This declaration is "not applicable".

References

[1] F. Chemat and M. K. Khan, "Applications of Ultrasound in Food Technology: Processing, Preservation and Extraction," *Ultrasonics Sonochemistry,* vol. 18, no. 4, pp. 813-835, 2011,
https://doi.org/10.1016/j.ultsonch.2010.11.023.

[2] B. Verhaagen, T. Zanderink, and D. F. Rivas, "Ultrasonic Cleaning of 3D Printed Objects and Cleaning Challenge Devices," *Applied Acoustics,* vol. 103, pp. 172-181, 2016, https://doi.org/10.1016/j.apacoust.2015.06.010.

[3] J. Yang and B. Cao, "Investigation of Resistance Heat Assisted Ultrasonic Welding of 6061 Aluminum Alloys to Pure Copper," *Materials & Design,* vol. 74, pp. 19-24, 2015, https://doi.org/10.1016/j.matdes.2015.02.028.

[4] S. Bagherzadeh, K. Abrinia, and Q. Han, "Ultrasonic Assisted Equal Channel Angular Extrusion (UAE) as a Novel Hybrid Method for Continuous Production of Ultra-fine Grained Metals," *Materials Letters,* vol. 169, pp. 90-94, 2016,
https://doi.org/10.1016/j.matlet.2016.01.095.

[5] J. Gallego-Juárez, G. Rodríguez, E. Riera, and A. Cardoni, "Ultrasonic Defoaming and Debubbling in Food Processing and Other Applications," in *Power Ultrasonics*: Elsevier, 2015, pp. 793-814.

[6] S. Amini, M. Soleimani, H. Paktinat, and M. Lotfi, "Effect of Longitudinal− torsional Vibration in Ultrasonic-assisted Drilling," *Materials and Manufacturing Processes,* vol. 32, no. 6, pp. 616-622, 2017, https://doi.org/10.1080/10426914.2016.1198027.

[7] M. Molaie, J. Akbari, and M. Movahhedy, "Ultrasonic Assisted Grinding Process with Minimum Quantity Lubrication Using Oil-based Nanofluids," *Journal of Cleaner Production,* vol. 129, pp. 212-222, 2016, https://doi.org/10.1016/j.jclepro.2016.04.080.

[8] M. R. Karafi and S. Korivand, "Design and Fabrication of a Novel Vibration-assisted Drilling Tool Using a Torsional Magnetostrictive Transducer," *The International Journal of Advanced Manufacturing Technology,* vol. 102, pp. 2095-2106, 2019, https://doi.org/10.1007/s00170-018-03274-w.

[9] D. Shahgholian Ghahfarokhi, M. Salimi, and M. Farzin, "Experimental Study of the Effect of Ultrasonic Vibrations on Sliding Friction Force in Longitudinal Direction," *Modares Mechanical Engineering,* vol. 15, no. 9, pp. 187-198, 2015, http://dorl.net/dor/20.1001.1.10275940.1394.15.9.22.4.

[10] J. Strobel, S. J. Rupitsch, and R. Lerch, "Ferroelectret Sensor Array for Characterization of Cavitation Effects in Ultrasonic Cleaning," in *2009 IEEE International Ultrasonics Symposium*, 2009: IEEE, pp. 1-4, 10.1109/ULTSYM.2009.5441745.

[11] R. Gopinath, A. K. Dalai, and J. Adjaye, "Effects of Ultrasound Treatment on the Upgradation of Heavy Gas Oil," *Energy & Fuels*, vol. 20, no. 1, pp. 271-277, 2006, https://doi.org/10.1021/ef050231x.

[12] C. Ruirun *et al.*, "Effects of Ultrasonic Vibration on the Microstructure and Mechanical Properties of High Alloying TiAl," *Scientific Reports*, vol. 7, no. 1, p. 41463, 2017, https://doi.org/10.1038/srep41463.

[13] C. E. Brennen, "Cavitation in Biological and Bioengineering Contexts," 2003.

[14] B. R. Munson, D. F. Young, and T. H. Okiishi, "Fundamentals of Fluid Mechanics," *Oceanographic Literature Review*, vol. 10, no. 42, p. 831, 1995.

[15] L. E. Kinsler, A. R. Frey, A. B. Coppens, and J. V. Sanders, "Fundamentals of Acoustics, John Wiley & Sons," *Inc, New York*, 2000.

Nomenclature

A	Contact surface	m^2
a	Booster's tip radius	m
c	Speed of sound	m/s
d_0	Booster's forehead diameter	m
F	Shear force	N
f	frequency	Hz
h	Amplitude of transverse vibrations	m
I	Motor current	A
k	Wave number	$1/m$
l	Amplitude of longitudinal vibrations	m
l_0	Length of the booster hole	m
M	Torque	$N.m$
P_A	Pressure amplitude	Pa
r_0	Booster hole radius	m
r	Distance from tip of the booster	m
T_m	Torque of DC motor	N.m
T	Periode of vibrations	s
V	Rotating surface speed	m/s
ν_0	Booster's tip velosity amplitude	m
r	Radial coordinate	m
ω	Frequency of vibration	Rad/s
φ	Magnetic flux	T
ρ	density	kg/m^3
μ	viscosity	$N.s/m^2$
τ	Shear stress	N/m^2
λ	wavelength	m
$\widetilde{\omega}$	Angular velosity of the shaft	rpm